JOURNAL OF SOLID STATE CHEMISTRY **139,** 79–84 (1998)
ARTICLE NO. SC987809

Synthesis, Characterization, and Magnetic Properties of New Rh(III) Compounds with the K_4CdCl_6 Structure-Type: Sr_3MRhO_6 (M = Sm, Eu, Tb, Dy, Ho, Er, and Yb)

Ralph C. Layland, Shalawn L. Kirkland, and Hans-Conrad zur Loye[1]

Department of Chemistry and Biochemistry, University of South Carolina, Columbia, South Corolina 29208

Received November 3, 1997; in revised form February 26, 1998; accepted March 3, 1998

The compounds Sr_3MRhO_6 (M = Sm, Eu, Tb, Dy, Ho, Er, and Yb) have been synthesized and structurally characterized by Rietveld refinement of powder X-ray diffraction data in the space group $R\bar{3}c$; $Z = 6$. The lattice parameters for the series were found to be $a = 9.78570(7)$ and $c = 11.4811(1)$ Å, $a = 9.7837(1)$ and $c = 11.4421(2)$ Å, $a = 9.7662(2)$ and $c = 11.3812(4)$ Å, $a = 9.7627(2)$ and $c = 11.3451(2)$ Å, $a = 9.7591(2)$ and $c = 11.3159(2)$ Å, $a = 9.7557(2)$ and $c = 11.2919(3)$ Å, and $a = 9.7390(2)$ and $c = 11.2501(3)$ Å, for Sr_3SmRhO_6, Sr_3EuRhO_6, Sr_3TbRhO_6, Sr_3DyRhO_6, Sr_3HoRhO_6, Sr_3ErRhO_6, and Sr_3YbRhO_6, respectively. These compounds are isostructural with K_4CdCl_6. The structure consists of infinite one-dimensional chains of alternating face-shared RhO_6 octahedra and MO_6 trigonal prisms (M = Sm, Eu, Tb, Dy, Ho, Er, and Yb). The strontium cations are located in a distorted square antiprismatic environment. Magnetic susceptibility data for the compounds Sr_3MRhO_6 (M = Tb, Dy, Ho, Er, and Yb) obey the Curie law, with the expected μ_{eff} values consistent with an oxidation state of +3 for both Rh and M. © 1998 Academic Press

Key Words: **Sr_3SmRhO_6; Sr_3EuRhO_6; Sr_3TbRhO_6; Sr_3DyRhO_6; Sr_3HoRhO_6; Sr_3ErRhO_6; Sr_3YbRhO_6; Rietveld refinement; oxides; rhodium(III); magnetic properties.**

INTRODUCTION

The investigation of one-dimensional oxides of the noble metals is of interest to chemists and physicists due to the structural and magnetic properties of these materials (1–4). We have reported the synthesis and characterization of a series of compounds in this family of materials. These compounds include Sr_3ZnMO_6 (M = Pt and Ir) (5), Sr_3MgMO_6 (M = Pt, Ir, and Rh) (6), and Ca_3NaMO_6 (M = Ru and Ir) (7). These, and related oxides which are isostructural with K_4CdCl_6 and have the general formula $A_3BB'O_6$ (8), are described as consisting of infinite chains of alternating face-shared octahedra [$B'O_6$] [B' = Pt, Ir, Rh, Nb, Ta, and Bi] and trigonal prisms [BO_6] [B = Na, Mg, Ca, Sr, Ba, Cu, Ni, Co, Zn, and Cd]. Each chain is surrounded by six parallel neighboring chains that are separated by A cations (A = alkali or alkaline earth cation). This structure type is extremely versatile and receptive to a large number of possible cationic substitutions; interesting magnetic properties have been observed. In numerous compounds, the oxidation states for the B and B' cations are +2 and +4, respectively (6). In addition, several compounds with oxidation states of +1 and +5, such as Sr_3NaRuO_6 (3), Ba_3LiBiO_6 (9), Ba_3NaBiO_6 (9), Ba_3NaNbO_6 (10), and Ba_3NaTaO_6 (10), are known. Conversely, only relatively few compounds with both cations in the +3 oxidation state occupying both the octahedral and trigonal prismatic sites have been prepared. Examples of compounds of this type include Sr_3YbNiO_6 (11), Sr_3MNiO_6 (M = Sc, In, Tm, Yb, and Lu) (12), and $Ca_3Co_2O_6$ (13). Recently, we reported the synthesis of the first examples of Rh(III) compounds with this structure type, Sr_3GdRhO_6, Sr_3YRhO_6, Sr_3ScRhO_6, and Sr_3InRhO_6, with both B and B' cations in the +3 oxidation state (14, 15).

In this paper we describe the further syntheses, structural characterizations, and magnetic properties of Rh(III) oxides with the general formula Sr_3MRhO_6, where M = Sm, Eu, Tb, Dy, Ho, Er, and Yb.

EXPERIMENTAL

Sample Preparation

Polycrystalline samples of Sr_3MRhO_6 (where M = Sm, Eu, Tb, Dy, Ho, Er, and Yb) were prepared by heating stoichiometric quantities of strontium carbonate (Alfa, 99.99%) with either samarium chloride hexahydrate (REacton, 99.99%), europium oxide (REacton, 99.9%), terbium chloride hexahydrate (Alfa, 99.99%), dysprosium chloride hexahydrate (Alfa, 99.99%), holmium(III) nitrate pentahydrate (Aldrich, 99.9%), erbium chloride hexahydrate (Alfa, 99.99%), or ytterbium oxide (REacton, 99.9%), and rhodium metal powder (Engelhard, 99.95%) at 1150°C for

[1]To whom correspondence should be addressed. Fax: (803) 777-9521. E-mail: hanno@psc.sc.edu.

0022-4596/98 $25.00

several days. The oxides, chlorides, or nitrates were first dissolved in approximately 100 ml of concentrated nitric acid in a Pyrex beaker. Once the rare-earth oxide, chloride, or nitrate was dissolved, the strontium carbonate and rhodium metal were added to the mixture. The reaction was stirred initially for one hour to ensure thorough mixing. Then, the reaction mixtures were heated with continued stirring until dryness. The dried reaction mixtures were initially heated in air overnight at 450°C in the Pyrex beaker. Subsequently, the samples were ground under acetone and transferred to an alumina crucible with a cover. All the compounds were synthesized following the same procedure. The alumina crucibles were heated at a rate of 25°C/min to 850°C, held at this temperature for 10 hours, and then heated at 10°C/min to 1150°C for 7–10 days with intermittent grindings. The samples were cooled at a rate of 10°C/min to room temperature. When the samples are prepared at 1150°C, the materials range in color from light to dark brown. Long thermal treatments at ≥ 1300°C lead to the decomposition of this phase. The rare-earth chlorides and nitrates were selected to produce single-phase products, since attempts to use only the rare-earth oxides as the starting reagents produced multiphase products.

Crystal Structure Determination

The X-ray powder diffraction data was collected on a Rigaku D\Max-2200 powder X-ray diffractometer using a Bragg-Brentano geometry with Cu$K\alpha$ radiation. Three step-scans were collected and summed. Small impurity peaks were found in all samples; however, they could not be identified. The step-scans covered the angular range 15°–115° 2θ in steps of 0.02° 2θ.

The structure refinements of Sr_3MRhO_6 (M = Sm, Eu, Tb, Dy, Ho, Er, and Yb) were carried out in the space group $R\bar{3}c$ (No. 167) using the structure of Sr_4PtO_6 (16, 17) as the starting model. Based on our recent experience with structurally related compounds, the rhodium atom was placed in the octahedral site 6*b*, the rare-earth atom was placed in the trigonal prismatic site 6*a*, and the strontium atom was placed in the 18*e* site. Structure refinements were performed using the Rietveld method (18) implemented in the computer program GSAS (19). The profile of the diffraction peaks of Sr_3MRhO_6 (M = Sm, Eu, Tb, Dy, Ho, Er, and Yb) was described by a pseudo-Voigt function. Refinements of the peak asymmetry were allowed, and the background was described by a polynomial function with six refineable coefficients. A total of 29 parameters, including six profile parameters, were used in the refinements. The results of the refinements are summarized in Table 1. Minor amounts of an impurity phase were observed in all samples, with the largest amount of the impurity phase in the Sr_3YbRhO_6 sample. Unfortunately, the impurity phase was not identified and therefore larger values of R_p and R_{wp} were obtained. We performed various refinements to check for antisite disorder and partial substitution of Al(III) (from the crucible) for Rh(III). The best refinement is obtained with the rare-earth metal in the 6*a* site and the rhodium in the 6*b*

TABLE 1
Summary of Crystallographic Data and Least-Squares Refinement Results for Sr_3MRhO_6 (M = Sm, Eu, Tb, Dy, Ho, Er, and Yb)

Compound	Sr_3SmRhO_6	Sr_3EuRhO_6	Sr_3TbRhO_6	Sr_3DyRhO_6	Sr_3HoRhO_6	Sr_3ErRhO_6	Sr_3YbRhO_6
a (Å)	9.78570(7)	9.7837(1)	9.7662(2)	9.7627(2)	9.7591(2)	9.7557(2)	9.7390(2)
c (Å)	11.4811(1)	11.4421(2)	11.3812(4)	11.3451(2)	11.3159(2)	11.2919(3)	11.2501(3)
V(Å^3)	952.13(2)	948.52(3)	940.10(6)	936.44(4)	933.33(4)	930.71(5)	924.10(6)
Observations	304	302	305	303	276	302	303
χ^2	2.492	3.398	6.103	4.354	4.649	4.880	3.527
R_p[a]	0.075	0.096	0.100	0.086	0.080	0.076	0.114
R_{wp}[a]	0.114	0.133	0.139	0.127	0.109	0.111	0.166
R_{exp}[a]	0.072	0.072	0.057	0.061	0.051	0.050	0.088
R_{Bragg}[a]	0.041	0.089	0.087	0.049	0.058	0.049	0.072

[a] Reliability factors were calculated as:

$$R_p = \sum |I_o - I_c| / \Sigma I_o$$

$$R_{wp} = [\sum w |I_o - I_c|^2 / \sum w I_o^2]^{1/2}$$

$$R_{exp} = R_{wp} / (\chi^2)^{1/2}$$

$$R_{Bragg} = \sum |I_{k(obs)} - I_{k(calc)}| / \sum I_{k(obs)}$$

where I_o and I_c are the observed and calculated integrated intensities, I_k is the Brass intensity, and w is the weight derived from an error propagation scheme during the process of least-squares refinement.

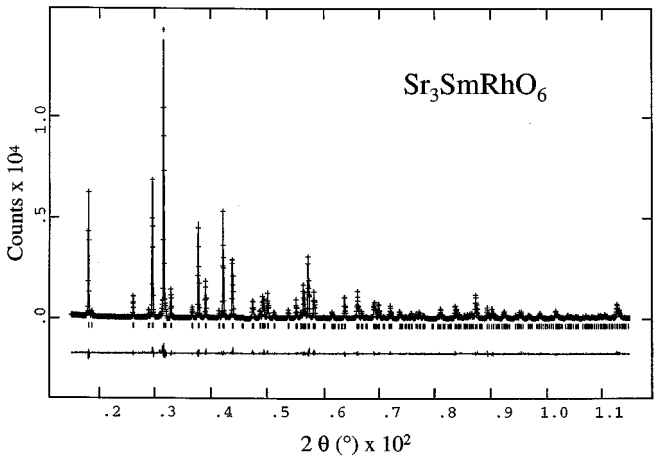

FIG. 1. Observed (cross) and calculated (solid line) X-ray diffraction patterns of Sr_3SmRhO_6. Tick marks indicate the positions of allowed Bragg reflections. The difference line, observed minus calculated, is located at the bottom of the figure.

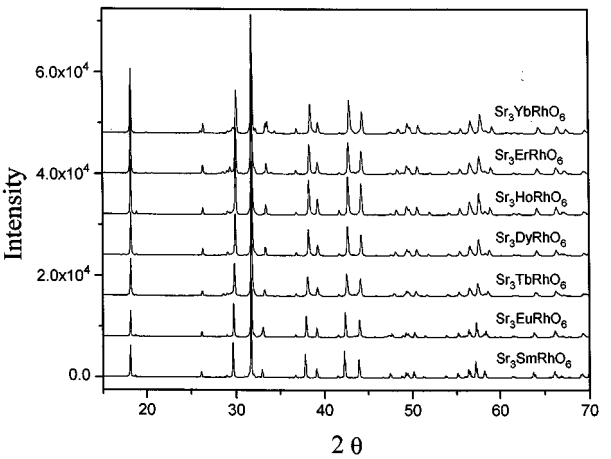

FIG. 2. Powder X-ray diffraction patterns of Sr_3MRhO_6 (M = Sm, Eu, Tb, Dy, Ho, Er, and Yb).

site with full occupancy for both metals. Nonetheless, we cannot rule out the possibility that a very slight (less than 800 ppm) substitution of aluminum for rhodium has occurred due to heating in alumina crucibles.

Magnetic Susceptibility Measurements

The magnetic susceptibilities of Sr_3MRhO_6 (M = Sm, Eu, Tb, Dy, Ho, Er, and Yb) were measured using a SQUID magnetometer in an applied field of 5000 G. The samples were first cooled to 5 K in a zero field, at which point a magnetic field was applied. The magnetization of the sample was then measured upon heating the sample from 5 to 300 K. The very small diamagnetic contribution of the sample holder was not corrected for due to its negligible contribution to the overall magnetization, which was dominated by the sample.

RESULTS AND DISCUSSION

Crystallographic data and further details of the Rietveld refinements of Sr_3MRhO_6 (M = Sm, Eu, Tb, Dy, Ho, Er, and Yb) are given in Table 1. The best agreement obtained between the calculated and observed profile patterns for Sr_3SmRhO_6 is shown in Fig. 1. The X-ray powder data for Sr_3MRhO_6, where M = Sm, Eu, Tb, Dy, Ho, Er, and Yb, are shown in Fig. 2. The atomic positions and thermal parameters for Sr_3MRhO_6, (M = Sm, Eu, Tb, Dy, Ho, Er, and Yb) can be found in Table 2. Selected interatomic bond distances and angles can be found in Table 3. Sr_3MRhO_6 (M = Sm, Eu, Tb, Dy, Ho, Er, and Yb) are isostructural with the rhombohedral structure type K_4CdCl_6, as was expected based on the fairly large number of compounds that have been synthesized with this structure type. The rhombohedral structure can be described as consisting of

TABLE 2
Atomic Positions Sr (x, 0, 1/4), M (0, 0, 1/4), Rh (0, 0, 0), and O (x, y, z) and Isotropic Thermal Parameters (Å²) (esds in Parentheses for Sr_3MRhO_6 (M = Sm, Eu, Tb, Dy, Ho, Er, and Yb))

	Sr_3SmRhO_6	Sr_3EuRhO_6	Sr_3TbRhO_6	Sr_3DyRhO_6	Sr_3HoRhO_6	Sr_3ErRhO_6	Sr_3YbRhO_6
Sr(x)	0.36986(9)	0.3688(1)	0.3690(1)	0.3696(1)	0.3690(1)	0.3690(1)	0.3689(2)
O(x)	0.1846(5)	0.1880(6)	0.1795(8)	0.1822(5)	0.1812(5)	0.1768(6)	0.1776(8)
O(y)	0.0256(6)	0.0239(7)	0.0225(9)	0.0240(6)	0.0225(5)	0.0212(7)	0.0193(9)
O(z)	0.1095(4)	0.1074(5)	0.1119(6)	0.1121(4)	0.1116(4)	0.1106(5)	0.1112(8)
Sr (U_{iso})	0.0034(5)	0.0023(7)	0.006(1)	0.0061(8)	0.0053(9)	0.0055(7)	0.0068(9)
M (U_{iso})	0.0040(6)	0.0082(7)	0.007(1)	0.0063(7)	0.0168(9)	0.0067(8)	0.0065(9)
Rh (U_{iso})	0.0015(6)	0.0014(7)	0.004(1)	0.0041(7)	0.0031(9)	0.0031(8)	0.0008(9)
O (U_{iso})	0.006(1)	0.007(2)	0.007(2)	0.006(2)	0.002(2)	0.008(2)	0.007(2)

TABLE 3
Interatomic Distances (Å) and Bond Angles (°) esds (in Parentheses) for Sr_3MRhO_6 (M = Sm, Eu, Tb, Dy, Ho, Er, and Yb)

	Sr_3SmRhO_6	Sr_3EuRhO_6	Sr_3TbRhO_6	Sr_3DyRhO_6	Sr_3HoRhO_6	Sr_3ErRhO_6	Sr_3YbRhO_6
M–O (×6)	2.340(4)	2.382(5)	2.283(7)	2.291(5)	2.289(4)	2.267(5)	2.267(8)
Rh–O (×6)	2.111(4)	2.125(5)	2.088(6)	2.102(4)	2.093(4)	2.054(5)	2.065(8)
Sr–O (×2)	2.531(4)	2.502(5)	2.520(6)	2.505(5)	2.503(4)	2.535(5)	2.509(7)
Sr–O (×2)	2.657(5)	2.672(6)	2.670(7)	2.664(5)	2.674(4)	2.677(5)	2.691(8)
Sr–O (×2)	2.752(5)	2.742(6)	2.736(8)	2.738(5)	2.728(4)	2.718(6)	2.697(8)
Sr–O (×2)	2.622(4)	2.576(5)	2.648(7)	2.663(5)	2.626(4)	2.632(5)	2.622(8)
O–M–O (×6)	77.7(2)	78.2(2)	77.8(3)	78.5(2)	78.3(2)	77.1(2)	77.8(3)
O–M–O (×3)	88.1(2)	87.4(2)	87.9(3)	87.0(2)	87.2(2)	88.7(3)	87.7(4)
O–M–O (×3)	127.8(2)	128.4(3)	128.6(4)	127.9(3)	128.5(2)	129.6(3)	130.0(4)
O–M–O (×3)	147.6(2)	146.5(3)	146.7(4)	146.8(3)	146.3(2)	146.4(3)	145.3(4)
M–O–Rh	80.1(1)	78.6(2)	81.1(2)	80.3(2)	80.3(1)	81.4(2)	80.5(2)
ϕ, Twist angle	14.7(1)	13.4(1)	13.2(1)	13.9(1)	13.1(1)	12.6(1)	11.4(1)

slightly bent chains of face-connected trigonal prisms and octahedra. A view of the unit cell looking down [001] can be seen in Fig. 3. The rhodium ions are located at the corners and center of the unit cell. Six equivalent oxygen ions are coordinated to the rhodium ion in an octahedral array at distances ranging from 2.054(5) Å for Er to 2.125(5) Å for Eu. The octahedral sites of oxides having this structure are typically occupied by a tetravalent metal, where the size of the octahedrally coordinated cation has a noticeable influence on the magnitude of the **c**-parameter. In our case, the trivalent cation, Rh(III) (0.67 Å), is larger than most of the tetravalent cations that have been found in the octahedral site, for instance Rh(IV) (0.60 Å), Ir(IV) (0.625 Å), and Pt(IV) (0.625 Å). This increase in the size is not, however, reflected in the **c**-parameter, which is also affected by the size of the metal in the trigonal prismatic site. The variation of V and c/a with M^{3+} ionic radius is shown in Fig. 4. The gadolinium ion, which we recently were able to place in the trigonal prismatic site, has an ionic radius of 0.938 Å. Since we were able to place the gadolinium ion into the trigonal prismatic site, substitution for the gadolinium ion was carried out using ions with similar or slightly smaller ionic radii. We were successful in substituting Sm (0.958 Å), Eu (0.947 Å), Tb (0.923 Å), Dy (0.912 Å), Ho (0.901 Å), Er (0.89 Å), and Yb (0.868 Å) (20) into the trigonal prismatic site. The scandium ion (0.745 Å) was the smallest $+3$ cation we were able to substitute into the trigonal prismatic site which could still stabilize the structure. Attempts to substitute ions smaller than Sc, such as Ga (0.62 Å), failed to stabilize this structure type. The rare-earth metal ions are coordinated in a trigonal prismatic array by six equivalent oxygens at distances ranging from 2.267(5) Å for Er to 2.382(5) Å for Eu. The trigonal prisms are distorted by a twist about the three-fold axis (ϕ). The twist angles, reported in Table 3, range from 11.4(1)° for Yb to 14.7(1)° for Sm. The trigonal prismatic coordination and the distortion about the three-fold axis can be seen more clearly in Fig. 5. The Sr–O bond distances are in agreement with those found in analogous compounds

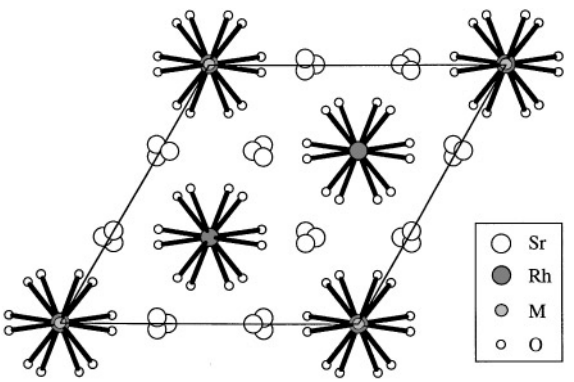

FIG. 3. A view of the unit cell of Sr_3MRhO_6 (M = Sm, Eu, Tb, Dy, Ho, Er, and Yb) in the *ab* plane looking down the metal oxide chains, which are separated by the strontium cations.

TABLE 4
Magnetic Data for Sr_3MRhO_6 (M = Sm, Eu, Tb, Dy, Ho, Er, and Yb) at 280 K

	μ_{theor} (22)	μ_{exp}	Ground state
Sr_3SmRhO_6	1.60	0.83	$^6H_{5/2}$
Sr_3EuRhO_6	3.61	3.30	$^7F_0$
Sr_3TbRhO_6	9.72	9.31	$^7F_6$
Sr_3DyRhO_6	10.63	10.37	$^6H_{15/2}$
Sr_3HoRhO_6	10.60	10.29	$^5I_8$
Sr_3ErRhO_6	9.57	9.26	$^4I_{15/2}$
Sr_3YbRhO_6	4.50	4.12	$^2F_{7/2}$

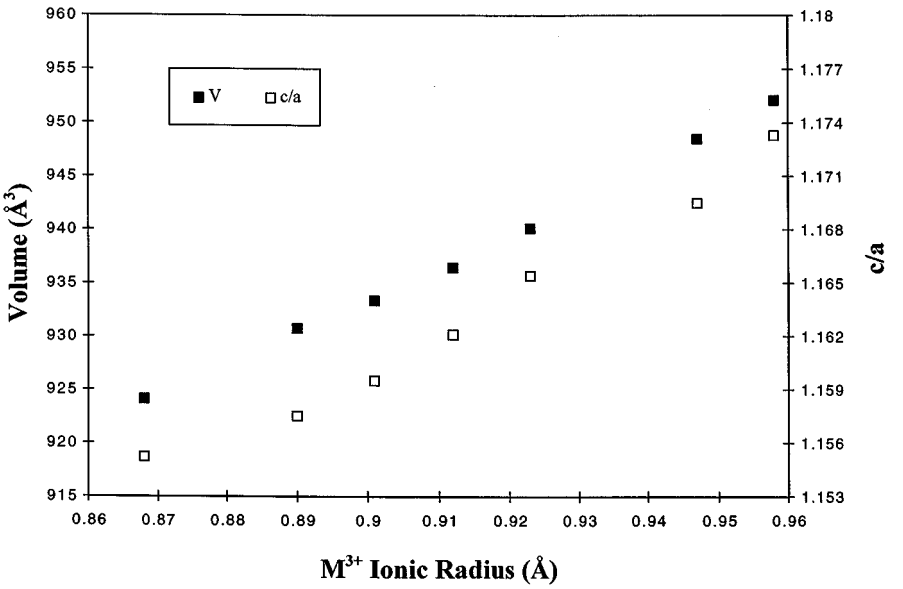

FIG. 4. The variation of the cell volume V (filled squares) and c/a (open squares) with M^{3+} ionic radius for Sr_3MRhO_6 (M = Yb, Er, Ho, Dy, Tb, Eu, and Sm) in order of increasing ionic radius.

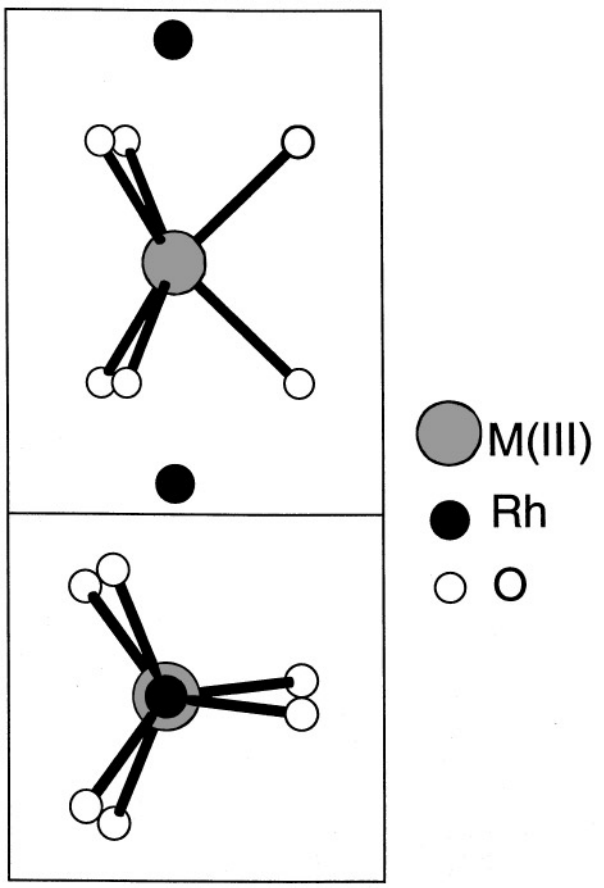

FIG. 5. The coordination environment around the trigonal prismatic metal site M, where M = Sm, Eu, Tb, Dy, Ho, Er, and Yb. The top portion shows the collinearity between the Rh and M sites along the chain, while the slight distortion of the trigonal prism viewed down the c axis can be seen in the bottom portion.

(6). Likewise, the Rh–O bond distances are in agreement with those found for Rh(III) in other oxides (21).

The temperature dependence of the inverse magnetic susceptibility data for Sr_3MRhO_6, (M = Tb, Dy, Ho, Er, and Yb) can be seen in Fig. 6. The inverse magnetic susceptibility vs temperature data of all the samples except Sr_3SmRhO_6 and Sr_3EuRhO_6 were fitted to a Curie law (22). The susceptibilities of Sr_3SmRhO_6 and Sr_3EuRhO_6 do not follow the Curie law due to thermal population of the low-lying excited states. No correction for the temperature independent paramagnetism (TIP) was made. The ground states, theoretical effective magnetic moments (μ_{theor}) (22), and experimental effective magnetic moments (μ_{exp}) for Sr_3MRhO_6 (M = Sm, Eu, Tb, Dy, Ho, Er, and Yb) can be found in Table 4. These values are in agreement with both the rhodium and the rare-earth metal being present in the trivalent oxidation state. Rhodium(III) is a d^6 ion, which is known to give a low-spin $t_{2g}^6e_g^0$ electronic configuration in oxides, and consequently, no paramagnetic contribution to the sample magnetization. The preparation and structural and magnetic characterization of other isostructural rhodium(III) compounds are in progress.

In summary, we have prepared and characterized the compounds Sr_3MRhO_6, (M = Sm, Eu, Tb, Dy, Ho, Er, and Yb), which crystallize with the $R\bar{3}c$ space group symmetry of the K_4CdCl_6 structure type. We succeeded in introducing and stabilizing rhodium(III) in this structure type. The $+3$ oxidation state for the rhodium ion and rare-earth ion was confirmed by the structural and magnetic data.

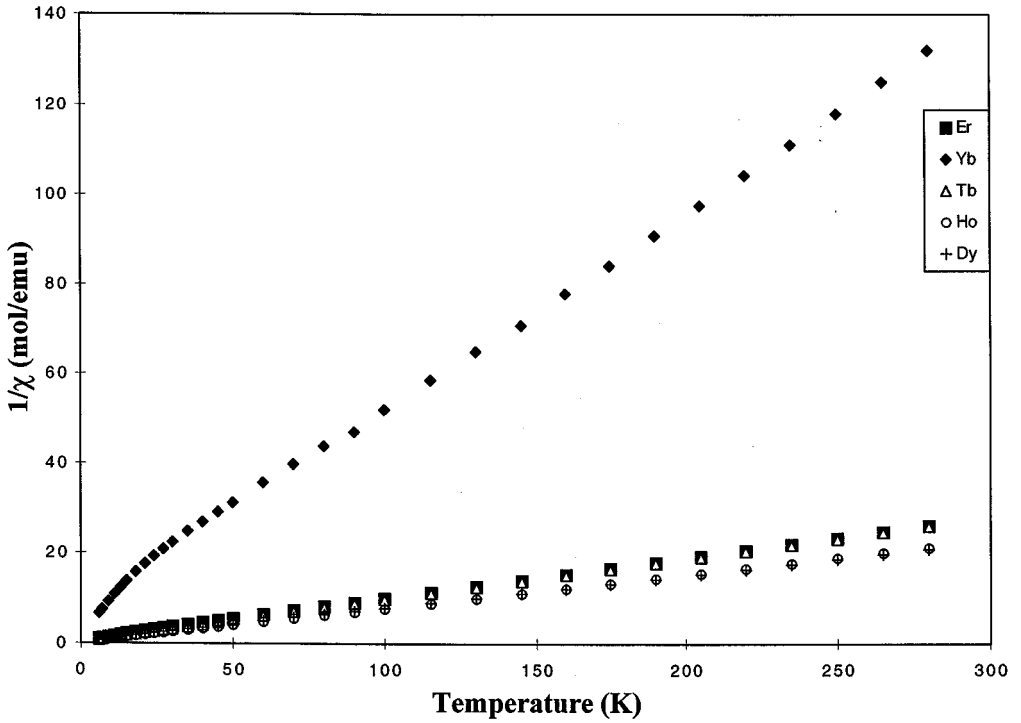

FIG. 6. Temperature dependence of the inverse magnetic susceptibility of Sr_3MRhO_6 (M = Tb, Dy, Ho, Er, and Yb), measured at 5000 G.

ACKNOWLEDGMENTS

Financial support was provided by the National Science Foundation through Grant DMR: 9696235. The funds used to purchase the powder X-ray diffractometer were provided by NSF/EPSCoR Cooperative Agreement EPS-9630167. We thank A. Stacy and B. Reisner at the University of California Berkeley for performing some of the magnetic measurements.

REFERENCES

1. T. N. Nguyen, D. M. Giaquina, and H.-C. zur Loye, *Chem. Mater.* **6,** 1624 (1994).
2. T. N. Nguyen and H.-C. zur Loye, *J. Solid State Chem.* **117,** 300 (1995).
3. S. Frenzen and H. Müller-Buschbaum, *Z. Naturforsch. B* **50,** 581 (1995).
4. J. F. Vente, J. K. Lear, and P. D. Battle, *J. Mater. Chem.* **5,** 1785 (1995).
5. C. Lampe-Önnerud, M. Sigrist, and H.-C. zur Loye, *J. Solid State Chem.* **127,** 25 (1996).
6. P. Núñez, S. Trail, and H.-C. zur Loye, *J. Solid State Chem.* **130,** 35 (1997).
7. J. B. Claridge, R. C. Layland, R. D. Adams, and H.-C. zur Loye, *Z. Anorg. Allg. Chem.* **623,** 1131 (1997).
8. G. Bergerhoff and O. Schmitz-Dumont, *Z. Anorg. Allg. Chem.* **284,** 10 (1956).
9. V. A. Carlson and A. M. Stacy, *J. Solid State Chem.* **96,** 332 (1992).
10. G. Wehrum and R. Hoppe, *Z. Anorg. Allg. Chem.* **617,** 45 (1992).
11. M. James and J. P. Attfield, *J. Mater. Chem.* **4,** 575 (1994).
12. M. James and J. P. Attfield, *Chem. Eur. J.* **216,** 737 (1996).
13. H. Fjellvåg, E. Gulbrandsen, S. Aasland, A. Olsen, and B. C. Hauback, *J. Solid State Chem.* **124,** 190 (1996).
14. P. Núñez, M. A. Rzeznik, and H.-C. zur Loye, *Z. Anorg. Allg. Chem.* **623,** 1269 (1997).
15. R. C. Layland, S. L. Kirkland, P. Núñez, and H.-C. zur Loye, *J. Solid State Chem.*, in press.
16. J. J. Randall and L. Katz, *Acta Crystallogr.* **2,** 519 (1959).
17. I. Ben-Dor, J. T. Suss, and S. Cohen, *J. Cryst. Growth* **64,** 395 (1983).
18. H. M. Rietveld, *J. Appl. Crystallogr.* **2,** 65 (1969).
19. A. C. Larson and R. B. Von Dreele, "General Structure Analysis System (GSAS)." Los Alamos National Laboratory Report No. LA-UR-86-748, 1994.
20. R. D. Shannon, *Acta Crystallogr. Sect. A* **32,** 751 (1976).
21. K. Hobbie and R. Hoppe, *Z. Anorg. Allg. Chem.* **535,** 20 (1986).
22. B. N. Figgis, "Introduction to Ligand Fields." Interscience Publishers, New York, 1966.